

Band-gap bowing in $\text{AgGa}(\text{Se}_{1-x}\text{Te}_x)_2$ and its effect on the second-order response coefficient and refractive indices

Chandrima Mitra and Walter R. L. Lambrecht

Department of Physics, Case Western Reserve University, Cleveland, Ohio 44106, USA

(Received 3 August 2007; revised manuscript received 11 October 2007; published 14 November 2007)

The quaternary chalcopyrite $\text{AgGa}(\text{Se}_{1-x}\text{Te}_x)_2$ alloy system is studied using the full-potential linearized muffin-tin orbital method and density functional theory in the local density approximation. Special quasirandom structures of 64-atom cells are used to model the disorder. Full structural relaxations were done in order to calculate the band gap for each concentration. The lattice parameters are found to vary almost linearly with concentration. The band gap bowing coefficient b was obtained to be 0.43 eV. The refractive indices and second harmonic generation coefficients are calculated as a function of Te concentration x , including a band gap correction. A small downward bowing is found for the indices of refraction and the birefringence, predicting a switch from negative to positive birefringence at about 67% Te. The second-order coefficients show a more pronounced and upward bowing, illustrating their stronger sensitivity to the band gap.

DOI: [10.1103/PhysRevB.76.205206](https://doi.org/10.1103/PhysRevB.76.205206)

PACS number(s): 71.20.Nr, 78.20.Ci, 71.15.Mb

I. INTRODUCTION

The $\text{AgGa}(\text{S}, \text{Se}, \text{Te})_2$ chalcopyrite crystals are of great practical interest in nonlinear optics.^{1,2} Since the chalcopyrite crystal structure is noncentrosymmetric, they possess a non-zero value of $\chi^{(2)}$ which can be quite large. The experimental values³ of $\chi^{(2)}$ for AgGaS_2 and AgGaSe_2 are 23 and 64 pm/V, respectively, while the experimental value for AgGaTe_2 is still to be determined. Moreover, the tetragonal crystal structure allows for birefringence, which can be used to achieve phase matching. These materials also have excellent transparency in the midinfrared range and are, thus, attractive for a variety of frequency conversion applications with target wavelengths in the midinfrared. The nonlinear optical coefficients were calculated by Rashkeev and Lambrecht,^{4,5} and these authors, in particular, emphasized the potential benefits of AgGaTe_2 , which was predicted to have a twice larger $\chi^{(2)}$ than AgGaSe_2 . Experimentally, AgGaTe_2 has received far less study than AgGaS_2 and AgGaSe_2 , but recently progress has been made in its crystal growth.^{6,7} Ohmer *et al.*² studied the birefringence in this material and found it to be positive in contrast to AgGaSe_2 . Thus, alloying between the two materials was proposed as an effective means to adjust the absolute value of the negative birefringence in AgGaSe_2 , in particular, so as to achieve the desired noncritical phase matching for specific frequency conversion purposes using popularly used lasers. It is, thus, important to be able predict how the index of refraction varies as a function of concentration. Previous work² simply assumed a linear dependence.

Therefore, the goal of this study is to calculate the band-gap bowing and its effect on the index of refraction and $\chi^{(2)}$ in the $\text{AgGa}(\text{Se}_{1-x}\text{Te}_x)_2$ alloy system. Also since $\chi^{(2)}$ increases rapidly with decreasing band gap, the variation of $\chi^{(2)}$ in the alloy system will be studied. In a broader context, the question of the origin of band-gap bowing remains of fundamental interest in semiconductor physics. Zunger and Jaffe⁸ have shown that most of the optical bowing in semiconductor alloys of the type $A_xB_{1-x}C$ is due to structural distortion, in particular, the local bond length adjustments.

Recently, we studied the band-gap bowing in $\text{Ag}_x\text{Cu}_{1-x}\text{GaS}_2$ alloys and found that the c/a ratio plays an important role. Mixed cation alloys have generally received more study than mixed anion systems. Thus, the present system $\text{AgGa}(\text{Se}_{1-x}\text{Te}_x)_2$ is also of interest because it is a mixed anion system. Among other mixed anion alloys studied before, Matsushita *et al.*⁹ have reported a concave decrease in the optical band gap with concentration in the $\text{AgGa}(\text{S}_{1-x}\text{Se}_x)_2$ system. On the other hand, Lee *et al.*¹⁰ have reported a linear variation of band gap in the same system. The band-gap bowing in the $\text{Cu}_x\text{Ag}_{1-x}\text{GaS}_y\text{Se}_{1-y}$ mixed cation and mixed anion systems was recently investigated computationally by Chen *et al.*¹¹ Therefore, here we focus exclusively on the $\text{AgGa}(\text{Se}_{1-x}\text{Te}_x)_2$ system.

II. COMPUTATIONAL APPROACH

The underlying computational approach is the density functional theory in the local density approximation.¹² The full-potential linear muffin-tin orbital (LMTO) method¹³ is used for structural relaxation and calculation of the band structures. The latter uses a basis set of smoothed Hankel functions.¹⁴ The Hankel function energies and smoothing radii, determining their overall decay and shape near the muffin-tin radius, respectively, were optimized so that a single set of functions per angular momentum $l=s, p, d$ can be used. The Ga 3d orbitals are treated as local orbitals,¹⁵ while the 4d orbitals are considered as valence orbitals. The Brillouin zone integrations are done using a shifted regular $4 \times 4 \times 4$ k-point mesh, symmetrized according to the crystal's point group.¹⁶

The average behavior of a random alloy is simulated by using the special quasirandom structures (SQS) approach.¹⁷ SQS are ordered structures whose correlation functions are close to the ensemble average of a random system. Thus, the average of quantities, which can be expanded in a truncated cluster expansion, can be reliably obtained. Specifically, we used 64-atom cells. The anions in this system form approximately a fcc lattice. Thus, our SQS consists of a 32-atom fcc

TABLE I. Short-range order Warren-Cowley parameters α_j for the 32-atom fcc SQS.

x	Neighbor shell j					
	1	2	3	4	5	6
1/4	0	0	-1/12	0	0	0
1/2	0	0	-1/8	0	0	0

binary alloy. Models were generated for five different values of x , namely, 0, 0.25, 0.5, 0.75, and 1, using a code provided by Ruban *et al.*¹⁸ The quality of the SQS is given by the deviations of the correlation functions from the random one, or for the pair correlation functions by the Warren-Cowley parameters,¹⁹ which should be as small as possible up to as large as possible neighbor distances. These are given in Table I. Our SQS are found to be equivalent to the ones in Chen *et al.*¹¹ For each of the compositions, the structures are fully relaxed before the band gaps are calculated. We also optimized the c/a ratio of the structures. Although it is not *a priori* obvious that band gaps can be well described by a cluster expansion approach underlying the SQS idea, SQS of fairly small size have been found to give good band gaps,^{11,17} which demonstrates the prime importance of local bonding configurations on band gaps in semiconductors. Thus, the 64-atom SQS cells are deemed large enough to describe band-gap bowing behavior.

The optical calculations are done in the atomic sphere approximation of the LMTO method. The band structures using this approach are checked to be in good agreement with the full-potential LMTO. Empty spheres are introduced as usual to cover the space with a close-packed arrangement of spheres. Since the optical parameters are sensitive to the band gaps, the calculated band gaps need to be adjusted in order to obtain the refractive index and the second harmonic coefficient. Band-gap corrections are first done to the end compounds AgGaSe₂ and AgGaTe₂. Adding direct scissor shifts did not provide sufficient accuracy, in particular, for calculating the nonlinear optical coefficients. Better agreement to experiment is obtained when corrections to the low lying conduction bands are applied at the level of the Hamiltonian by adding shifts to the s -orbital center of the band parameters, so that the eigenvectors are consistent with the eigenvalues as shown by Rashkeev *et al.*²⁰ Shifting the Ag s states had little effect on opening up the gap, while shifting the Ga s states and the empty sphere s states nearest to the gallium atoms did open up the band gap, in agreement with Rashkeev and Lambrecht.^{4,5} This is consistent with the orbital character of the bands near the conduction band minimum as was shown recently to be also the case in Cu _{x} Ag_{1- x} GaS₂ alloys.²¹ After the end compounds are matched with the experimental values, the same shifts are added to the alloy potential parameters. This correction is more or less constant across the Se-Te concentration range because the contribution of Ga s is not changing appreciably. Thus, it is not expected to contribute to the bowing. It does, however, affect the calculation of optical properties.

One might expect there to be other changes in the band structure beyond local density approximation (LDA). For ex-

TABLE II. Calculated properties of the end compounds AgGaSe₂ and AgGaTe₂.

	AgGaSe ₂		AgGaTe ₂	
	Theory	Expt. ^a	Theory	Expt.
a (Å)	5.985	5.98	6.297	6.29
c/a	1.816	1.82	1.862	1.87
u	0.2777		0.2679	
E_g (eV)	0.16	1.83	0.13	1.36 ^b

^aExperimental data from Ref. 26.

^bFrom Ref. 27.

ample, Ga $3d$ states might be expected to be shifted down. However, these shifts have only a small effect on the gap region because the Ga $3d$ bands are relatively deep. One might also expect the Ag d states, which have an important contribution to the valence band maximum (VBM), to shift down. However, whether we shift the VBM down or the conduction band minimum up should not affect how the gap behaves as a function of Se-Te composition. For the optical properties that concern us here, the important point is to adjust the corrections so as to obtain the correct gap for the end compounds.

In order to calculate the refractive index, first, the imaginary part of the linear dielectric constant is calculated using the expression (in Gaussian units)

$$\epsilon_2^j(\omega) = \left(\frac{2\pi e}{m\omega} \right)^2 \sum_{\mathbf{k}v\mathbf{c}} |\langle v\mathbf{k} | -i\hbar\nabla_j | c\mathbf{k} \rangle|^2 \delta[E_c(\mathbf{k}) - E_v(\mathbf{k}) - \hbar\omega]. \quad (1)$$

This expression is obtained in the random phase approximation long-wavelength limit. It, thus, neglects local field and excitonic effects. The real part of ϵ is obtained using the Kramers-Kronig relation, and finally, the refractive index is calculated by taking the real part of $\sqrt{\epsilon(\omega)}$. In doing the above calculations, the energy range is chosen from 0 to 27 eV, the k -point integration is done using the tetrahedron method,²² and a well converged fine mesh of $10 \times 10 \times 10$ k points is used for the supercells.

For the chalcopyrite crystal, the only nonzero $\chi^{(2)}$ coefficients are $\chi_{x,y,z}^{(2)}$ and $\chi_{z,x,y}^{(2)}$, which are equal in the static limit by the Kleinman symmetry.²³ The formalism followed for the calculation of $\chi^{(2)}$ was developed by Sipe and co-workers^{24,25} and implemented in LMTO by Rashkeev *et al.*²⁰ The same basic approximations as for the linear optics calculation are used, i.e., local field and excitonic effects are neglected. In this approach, the total $\chi^{(2)}$ is divided in a pure interband and mixed intraband-interband contribution, which we shall call intraband for short. For the end compounds, in the standard unit cell, a mesh of $15 \times 15 \times 15$ was found necessary to converge the $\chi^{(2)}$.

III. RESULTS

We begin with the end compounds of the series. In Table II, we show the calculated minimum energy lattice constants,

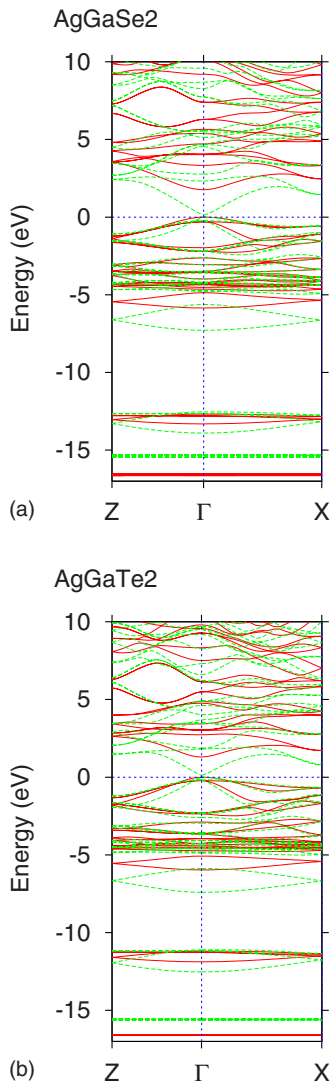


FIG. 1. (Color online) Band structure of (a) AgGaSe_2 and (b) AgGaTe_2 with (solid red line) and without (dashed green line) gap correction, $Z=(0,0,2\pi/c)$, and $X=(2\pi/a,0,0)$.

a , $c/a=2\eta$, and u for the end compounds as well as their band gap. The internal structural parameter u is defined by the bond lengths:

$$d_{AC} = a \sqrt{\left(\frac{1}{4}\right)^2 + u^2 + \frac{\eta^2}{4}},$$

$$d_{BC} = a \sqrt{\left(\frac{1}{4}\right)^2 + \left(\frac{1}{2} - u\right)^2 + \frac{\eta^2}{4}}. \quad (2)$$

The maxima of the valence band and the minima of the conduction band are found at the Γ point, giving a direct band gap in both cases. The experimental band gaps given in the table are low temperature gaps at 77 K. The lattice constants are in good agreement with experiment, and the gaps are, as usual, underestimated severely by the LDA. Both the selenide and telluride have a significant distortion of the c/a

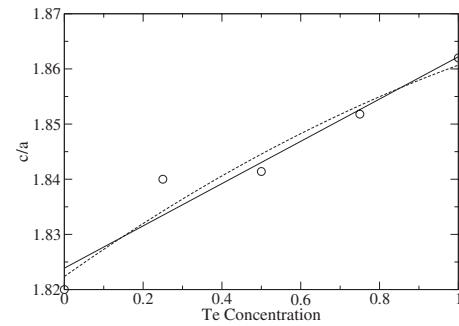


FIG. 2. Variation of the lattice parameter c/a with the Te concentration x in $\text{AgGa}(\text{Te}_x\text{Se}_{1-x})_2$. Solid line, linear fit; dashed line, quadratic fit.

and u from the ideal values 2 and 0.25. Also, both a and c/a increase from the selenide to the telluride.

The effects of the Ga s shift on the band structure of AgGaSe_2 and AgGaTe_2 are shown in Fig. 1. We may note that besides the gap increase, the bands are also affected in the region of about -6 eV. This is because the states in this energy range are Ga s -Se (or Te) p bonding states. Also, the Se s -Ga s bonding states at about -13 eV are affected. The lowest set of bands in the figure are the Ga $3d$ bands. These shift down slightly, which is an indirect effect of the self-consistency. The reduced Ga s charge in the spheres, resulting from their upward shift, leads to a reduced screening of the nuclear potential, which, in turn, shifts the Ga $3d$ states down. This is a shift in the right direction from what one expects the quasiparticle eigenvalues to do, even without adding an explicit $3d$ shift. If we further shift the Ga $3d$ states down by about 3 eV, the gap region is only affected by about 0.04 eV, so we decided not to include such shifts.

In Fig. 2, we show the behavior of c/a as a function of concentration since it was found to play an important role in the band-gap behavior in $\text{Cu}_{1-x}\text{Ag}_x\text{GaS}_2$ in Ref. 21. In the present case, c/a is found to vary linearly: within the error bars, there is no significant improvement in fit by adding a quadratic term. Also, c and a are found to vary linearly to very good approximation. Thus, Vegard's law is well obeyed in this case.²⁸

The optical band gap is plotted as a function of x in Fig. 3. In order to find the bowing parameter, the curve in Fig. 3 is fitted to the following equation:²⁹

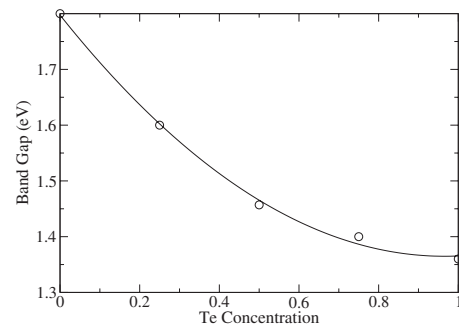


FIG. 3. Optical band gap as function of Te concentration x .

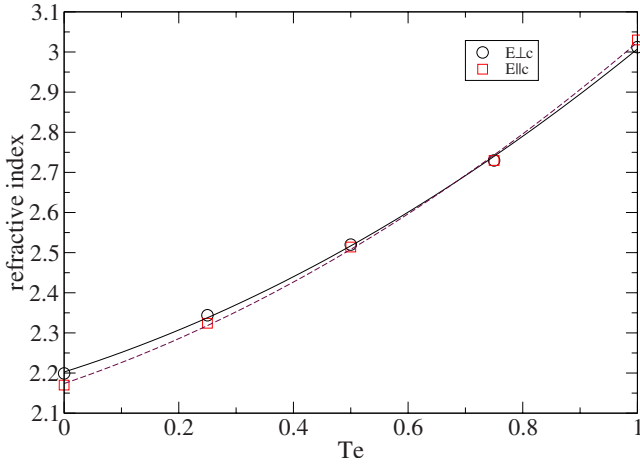


FIG. 4. (Color online) The variation of refractive indices with concentration (black solid line, $E \perp c$ or ordinary index; red dashed line, $E \parallel c$ or extraordinary index).

$$E_g(x) = (1-x)E_g(0) + xE_g(1) - bx(1-x), \quad (3)$$

where b is the bowing parameter and $E_g(x)$ is the band gap as a function of Te concentration x . The value of b obtained here is 0.43 eV. A positive value of b implies a downward bowing. This band-gap bowing is relatively small compared to that found in the $\text{Cu}_x\text{Ag}_{1-x}\text{GaS}_2$ system,²¹ but not negligible.

The ordinary and extraordinary refractive indices, in the static limit, are plotted as a function of x in Fig. 4. Interestingly, the indices of refraction show a small downward bowing. While the index of refraction is expected to behave inversely proportional to the interband differences, one might have expected an upward bowing if the gap bows downward. However, the index of refraction is not necessarily dominated by the lowest band gap. This illustrates that one cannot simply assume a linear dependence for indices of refraction. The switching of negative birefringence in AgGaSe_2 to positive birefringence of AgGaTe_2 is clearly reflected in the plot. From the plot of the birefringence in Fig. 5, it can be estimated to occur at about 67% concentration of Te.

The absolute values of our indices of refraction are underestimated for AgGaSe_2 and overestimated for AgGaTe_2 compared to experiment. Our calculation does not include dispersion resulting from the phonon absorptions. Therefore, we

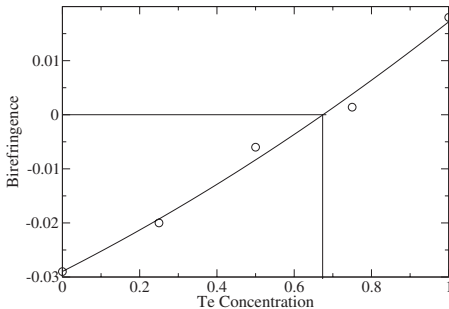


FIG. 5. The variation of birefringence with Te concentration.

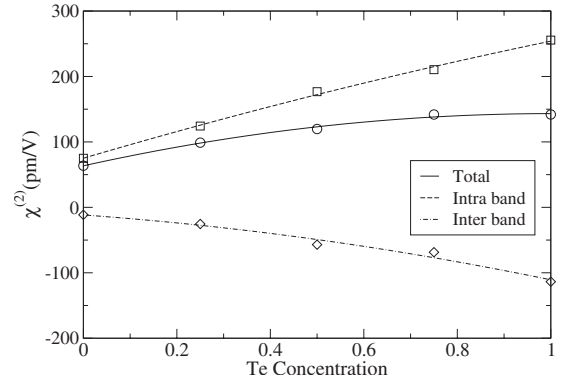


FIG. 6. The variation of $\chi^{(2)}$ and its inter- and intraband contributions with Te concentration.

compare our results with the values obtained from the Sellmeyer equation $n^2 = A + B\lambda^2/(\lambda^2 - C) + D\lambda^2/(\lambda^2 - E)$, fitted to the experimental data as function of wavelength λ . Here, the second term describes the dispersion resulting from electronic transitions, and the last term describes the dispersion resulting from phonon absorption. Thus, our calculated values correspond to taking the limit $\lambda \rightarrow \infty$ when neglecting the last term. In other words, $n = \sqrt{A+B}$. This gives $n_o = 2.617$ and $n_e = 2.586$ for AgGaSe_2 using data from Ref. 26, while our calculated values are $n_o = 2.199$ and $n_e = 2.170$. For AgGaTe_2 , the data from Ohmer *et al.*² give $n_o = 2.97$ and $n_e = 2.99$, while we obtain $n_o = 3.012$ and $n_e = 3.03$. These discrepancies most likely result from our neglect of local field effects and the manner in which the gap is corrected. It is somewhat puzzling why we underestimate the values by 20% for the selenide, but overestimate them by 1% in the telluride. In spite of these discrepancies on the absolute values, we obtain good agreement for the birefringence $n_e - n_o$, for which we find 0.018 and -0.029 in AgGaTe_2 and AgGaSe_2 , respectively, while the experiments give 0.02 and -0.031 . Thus, changes in indices of refraction seem to be much better than the absolute values.

The second harmonic generation coefficient and its separation into inter- and intraband contributions are plotted as a function of Te concentration in Fig. 6. Since the expressions for the second-order nonlinear coefficients contain terms that vary as the inverse square of the band gap,²⁰ it is more sensitive to the band-gap variation. Hence, its nonlinear behavior with concentration is more pronounced. As expected from a downward bowing of the gap, the $\chi^{(2)}$ bows upward. The intraband contribution appears to be nearly linear, but the interband contribution shows an upward bowing. For the end compounds, our values are in good agreement with previous calculations by Rashkeev and Lambrecht^{4,5} even though we used a slightly different way of adjusting the band gap here. For AgGaSe_2 , our value is 63.7 pm/V compared to 65.5 pm/V in Ref. 5 and experimental values ranging from 64 to 68 pm/V.^{3,30,31} For AgGaTe_2 , our value is 142 pm/V, while the Rashkeev-Lambrecht value is 138 pm/V.

IV. CONCLUSIONS

In this paper, we investigated the structural parameters and band-gap bowing and its effect on linear and nonlinear

optical parameters for $\text{AgGa}(\text{Se}_{1-x}\text{Te}_x)_2$ using first-principles calculations. A relatively small bowing parameter of 0.46 eV was found. Somewhat surprisingly, the indices of refraction and the birefringence also show a slight downward rather than upward bowing. Previous analysis² of the optimal concentrations for noncritical phase matching for CO_2 laser frequency doubling was based on the assumption of linear variation of the indices of refraction. The present results indicate that this assumption is not strictly valid. Fortunately, the bowing of the indices is relatively small so that the previous analysis still provides a reasonable estimate. To predict quantitatively the indices of refraction as a function of concentration in the appropriate wavelength regime, our present calculations are unfortunately not sufficiently accurate because one needs to also take into account the contributions from the phonons to the dispersion of the indices of refrac-

tion and correct for the local field effects. We found a slight upward bowing of the $\chi(2)$ with concentration. This implies that even with a small concentration of Te, one will benefit from a higher $\chi^{(2)}$. Our results show that this common cation system behaves very differently from the common anion $\text{Cu}_x\text{Ag}_{1-x}\text{GaS}_2$ alloys, which showed significantly larger bowing, mostly because of the deviations from Vegard's law for the c lattice constant.

ACKNOWLEDGMENTS

The work was supported by the Air Force Office of Scientific Research under Grant No. F49620-03-1-0010. Calculations were carried out using resources from the Ohio Supercomputer Center and the CWRU high-performance computing cluster.

-
- ¹G. C. Catella and D. Burlage, *Mater. Res. Bull.* **23**, 28 (1998), and references therein.
- ²M. C. Ohmer, J. T. Goldstein, D. E. Zelmon, A. Waxler, S. M. Hegde, J. D. Wolf, P. G. Schunemann, and T. M. Pollak, *J. Appl. Phys.* **86**, 94 (1999).
- ³J. L. Shay and J. H. Wernick, *Ternary Chalcopyrite Semiconductors: Growth, Electronic Properties, and Applications* (Pergamon, Oxford, 1975).
- ⁴S. N. Rashkeev and W. R. L. Lambrecht, *Appl. Phys. Lett.* **77**, 190 (2000).
- ⁵S. N. Rashkeev and W. R. L. Lambrecht, *Phys. Rev. B* **63**, 165212 (2001).
- ⁶A. Burger, J. O. Ndap, Y. Cui, U. Roy, S. Morgan, K. Chattopadhyay, X. Ma, K. Faris, S. Thibaud, R. Miles, H. Mateen, J. T. Goldstein, and C. J. Rawn, *J. Cryst. Growth* **225**, 505 (2001).
- ⁷U. N. Roy, B. Mekonen, O. O. Adetunji, K. Chattopadhyay, F. Kochari, Y. Cui, A. Burger, and J. T. Goldstein, *J. Cryst. Growth* **241**, 135 (2002).
- ⁸A. Zunger and J. E. Jaffe, *Phys. Rev. Lett.* **51**, 662 (1983).
- ⁹H. Matsushita, O. Shiono, S. Endo, and T. Irie, *Jpn. J. Appl. Phys., Part 1* **34**, 5546 (1995).
- ¹⁰M.-H. Lee, C.-H. Yang, and J.-H. Jan, *Phys. Rev. B* **70**, 235110 (2004).
- ¹¹S. Chen, X. G. Gong, and Su-Huai Wei, *Phys. Rev. B* **75**, 205209 (2007).
- ¹²P. Hohenberg and W. Kohn, *Phys. Rev.* **136**, B864 (1964); W. Kohn and L. J. Sham, *Phys. Rev.* **140**, A1133 (1965).
- ¹³M. Methfessel, M. van Schilfgaarde, and R. A. Casali, in *Electronic Structure and Physical Properties of Solids, The Uses of the LMTO Method*, edited by Hugues Dreyssé, Springer Lecture Notes, Workshop Mont Saint Odille, France, 1998 (Springer, Berlin, 2000), pp. 114–147.
- ¹⁴E. Bott, M. Methfessel, W. Krabs, and P. C. Schmidt, *J. Math. Phys.* **39**, 3393 (1998).
- ¹⁵D. Singh, *Phys. Rev. B* **43**, 6388 (1991).
- ¹⁶H. J. Monkhorst and J. D. Pack, *Phys. Rev. B* **13**, 5188 (1976).
- ¹⁷A. Zunger, S.-H. Wei, L. G. Ferreira, and J. E. Bernard, *Phys. Rev. Lett.* **65**, 353 (1990).
- ¹⁸A. V. Ruban, S. I. Simak, S. Shallcross, and H. L. Skriver, *Phys. Rev. B* **67**, 214302 (2003).
- ¹⁹J. M. Cowley, *J. Appl. Phys.* **21**, 24 (1950).
- ²⁰S. N. Rashkeev, W. R. L. Lambrecht, and B. Segall, *Phys. Rev. B* **57**, 3905 (1998).
- ²¹C. Mitra and W. R. L. Lambrecht, *Phys. Rev. B* **76**, 035207 (2007).
- ²²P. E. Blöchl, O. Jepsen, and O. K. Andersen, *Phys. Rev. B* **49**, 16223 (1994).
- ²³D. A. Kleinman, *Phys. Rev.* **126**, 1977 (1962).
- ²⁴J. E. Sipe and E. Ghahramani, *Phys. Rev. B* **48**, 11705 (1993).
- ²⁵C. Aversa and J. E. Sipe, *Phys. Rev. B* **52**, 14636 (1995).
- ²⁶A. MacKinnon, in *Ternary Semiconductors*, edited by O. Madelung, Landolt-Börnstein, New Series, Group III, Vol. 17, Pt. H (Springer, Berlin, 1985).
- ²⁷B. Tell, J. M. Shay, and H. M. Kasper, *Phys. Rev. B* **9**, 5203 (1974).
- ²⁸L. Vegard, *Z. Phys.* **5**, 17 (1921).
- ²⁹M. Cardona, *Phys. Rev.* **129**, 69 (1963).
- ³⁰S. K. Kurtz, J. Jerphagnon, and M. M. Choy, in *Elastic, Piezoelectric, Pyroelectric, Piezooptic, Electrooptic Constants, and Nonlinear Dielectric Susceptibilities of Crystals*, edited by K.-H. Hellwege and A. M. Hellwege, Landolt-Börnstein, New Series, Group III, Vol. 11 (Springer, Berlin, 1979).
- ³¹D. A. Roberts, *IEEE J. Quantum Electron.* **27**, 142 (1992).